Biomass burning related ozone damage on vegetation over the Amazon forest: A model sensitivity study.

F. Pacifico[1], G. A. Folberth[2], S. Sitch[3], J. M. Haywood[1,2], L. V. Rizzo[5], F. F. Malavelle, and P. Artaxo[4]

[1] College of Engineering, Mathematics and Physical Sciences, University of Exeter, Exeter, UK
[2] Met Office Hadley Centre, Exeter, UK
[3] Geography, College of Life and Environmental Sciences, University of Exeter, Exeter, UK
[4] Department of Applied Physics, Institute of Physics, University of Sao Paulo, Sao Paulo, Brazil
[5] Department of Earth and Exact Sciences, Institute of Environmental, Chemical and Pharmaceutics Sciences, Federal University of Sao Paulo, Sao Paulo, Brazil

Abstract

The HadGEM2 Earth System climate model was used to assess the impact of biomass burning on surface ozone concentrations over the Amazon forest and its impact on vegetation, under present-day climate conditions. Here we consider biomass burning emissions from wildfires, deforestation fires, agricultural forest burning, residential and commercial combustion. Simulated surface ozone concentration is evaluated against observations taken at two sites in the Brazilian Amazon forest for years 2010 to 2012. The model is able to reproduce the observed diurnal cycle of surface ozone mixing ratio at the two sites, but overestimates the magnitude of the monthly averaged hourly measurements by 5-15 ppb for each available month at one of the sites. We vary biomass burning emissions over South America by +/-20, 40, 60, 80 and 100% to quantify the modelled impact of biomass burning on surface ozone concentrations and ozone damage on vegetation productivity over the Amazon forest. We used the ozone damage scheme in the "high" sensitivity mode to give an upper limit for this effect. Decreasing South American biomass burning emissions by 100% (i.e. to zero) reduces surface ozone concentrations (by about 15ppb during the biomass burning season) and suggests a 15% increase in monthly mean net primary productivity averaged over the Amazon forest, with local increases up to 60%. The simulated impact of ozone damage from present-day biomass burning on vegetation productivity is about 230 TgC/yr. Taking into account that

uncertainty in these estimates is substantial, this ozone damage impact over the Amazon forest is of the same order of magnitude as the release of carbon dioxide due to fire in South America; in effect to potentially double the impact of biomass burning on the carbon cycle.

Introduction

Biomass burning is a global source of aerosol and trace gases, including ozone (O_3) precursors, and can lead to local and regional O_3 pollution. Tropospheric O_3 is a greenhouse gas and, above background concentrations, an air pollutant: it is harmful to human health (e.g. Lippmann 1993; Burnett et al., 1997) and it damages plants (e.g. Rich et al., 1964; Fiscus et al., 2005; Felzer et al., 2007; Ainsworth et al., 2012). Tropospheric O_3 is a product of photochemical reactions whose main precursors are nitrogen oxides (NO_x), carbon monoxide (CO), methane (CH_4) and volatile organic compounds (VOCs) (Seinfeld and Pandis, 1998). VOCs are particularly important in Amazonia because of the large natural biogenic and biomass burning emissions (Karl et al., 2007).

In the Amazon forest, biomass burning is mostly anthropogenic, and mainly occurs during the dry season (August to October). Biomass burning emissions drastically change the composition of the atmosphere, e.g. diurnal maximum mixing ratios of tropospheric O_3 varies from 12 parts per billion (ppb), during the wet season, to values as high as 100 ppb in the biomass burning affected dry season (Kirkman et al., 2002, Sigler et al., 2002, Artaxo et al., 2002, 2005, Rummel et al., 2007).

Surface O_3 mixing ratios over 40 ppb are known to produce visible leaf injury and damage to plants, reducing crop productivity and posing a threat to food security; nonetheless different climatic conditions (e.g. soil moisture and water stress) also play a role in determining leaf stomatal closure and hence there will be variable impacts of the same O_3 concentrations (Ashmore, 2005), e.g. tropical rainforest vegetation may be particularly sensitive to surface O_3, even at concentrations below 40ppb (a threshold associated with extra-tropical vegetation), due to high stomatal conductances. Moreover, tropical vegetation evolved in low background O_3 concentrations and could be more sensitive to O_3. In leaves, cellular damage caused by O_3 not only reduces photosynthetic rates but also requires increased resource allocation to detoxify and repair leaves (Ainsworth et al., 2012). Ozone damage to vegetation reduces plant productivity, decreasing the amount of carbon absorbed by plants, hence has an impact on climate via and indirect radiative forcing (Sitch et al., 2007).

Tropical rain forests play an important role in the global carbon budget, as they cover 12% of the Earth's land surface and contain around 40% of the terrestrial biosphere's carbon (Ometto et al., 2005, Taylor & Lloyd, 1992). It has been estimated that they may account for as much as 50% of

72 the global net primary productivity (Grace et al., 2001). Depending on age, land use and large scale
73 meteorological conditions, tropical forest ecosystems can act as net carbon sources, sinks, or they
74 can be in approximate balance (Lloyd. et al., 2007, Gatti et al., 2013), but it is uncertain if global
75 environmental changes are forcing these ecosystems outside their range of natural variation (Sierra
76 et al., 2007). However, biomass burning may further reduce natural sinks in the neighbouring intact
77 forest, via air pollution and O_3 damage on vegetation, and thus current estimates of the effects of
78 biomass burning on the carbon cycle (Le Quéré et al., 2009) may be underestimated. Biomass
79 burning is also an important aerosol source: regional levels of particulate matter are very high in the
80 dry season in Amazonia (Artaxo et al., 2013), and the increase in diffuse radiation due to changes in
81 aerosol loadings can increase net ecosystem exchange (NEE) quite significantly (Oliveira et al.,
82 2007, Cirino et al., 2013). After a certain level of aerosol optical depth, the decrease in radiation
83 fluxes can reduce significantly NEE over Amazonia (Cirino et al., 2013). This study does not
84 consider the effects of the changes in diffuse radiation due to biomass burning on photosynthesis, or
85 the impact of aerosols on O_3 chemistry via changing photolysis rate. That will be the focus of a
86 separate study. Our specific aim is to estimate the effect of O_3-induced changes on vegetation
87 productivity due to biomass burning.
88
89 Importantly, Sitch et al. (2007) performed their assessment of the potential impact of O_3 on
90 vegetation using an offline simulation where monthly mean O_3 concentrations derived with a global
91 chemistry climate model were used in determining the impacts of O_3 damage. Here we use an
92 online flux-gradient approach to quantify the impact of biomass burning on surface O_3
93 concentration and O_3 damage on vegetation over the Amazon forest (see model description). The
94 HadGEM2 (Hadley Centre Global Environment Model 2; Collins et al., 2011; Martin et al., 2011)
95 Earth System climate model is used to study these interactions. We show results of the evaluation of
96 surface O_3 simulated with HadGEM2 against observations in the Amazon forest and model
97 experiments quantifying the impact of biomass burning on plant productivity.
98
99
100 **Methods**
101
102 We used HadGEM2 to simulate surface O_3 concentrations and O_3 damage on vegetation for present-
103 day (2001-2009) climate conditions. Our version of HadGEM2 includes the O_3 damage scheme
104 developed by Sitch et al. (2007). We evaluated simulated surface O_3 against observations taken at
105 two sites in the Amazon forest: Porto Velho (Brazil; 8.69∞S; 63.87∞W), a site heavily impacted by

106 biomass burning emissions, and site ZF2 in the Cuieiras forest reserve in Central Amazonia (Brazil;
107 2.59∞S; 60.21∞W). A description of the sites can be found in Artaxo et al. (2013). In a sensitivity
108 study we varied biomass burning emissions over South America by +/-20, 40, 60, 80, 100% to
109 quantify the potential impact of biomass burning on surface O_3 concentrations and O_3 damage over
110 the Amazon forest.
111
112
113 **Model description**
114
115 HadGEM2 is a fully coupled Earth-system model (Collins et al., 2011). It is built around the
116 HadGEM2 atmosphere-ocean general circulation model and includes a number of earth system
117 components: the ocean biosphere model diat-HadOCC (Diatom-Hadley Centre Ocean Carbon
118 Cycle, a development of the HadOCC model of Palmer and Totterdell, 2001), the Top-down
119 Representation of Interactive Foliage and Flora Including Dynamics (TRIFFID) dynamic global
120 vegetation model (Cox, 2001), the land-surface and carbon cycle model MOSES2 (Met Office
121 Surface Exchange Scheme; Cox et al. 1998, 1999; Essery et al. 2003), the interactive Biogenic
122 Volatile Organic Compounds (iBVOC) emission model (Pacifico et al., 2012), the United Kingdom
123 Chemistry and Aerosol (UKCA) model (O'Connor et al., 2014) and an interactive scheme of O_3
124 damage on vegetation (Sitch et al., 2007; Clark et al., 2011).
125
126 The configuration used here is a version of HadGEM2-UKCA with extended tropospheric
127 chemistry (N96L38), the resolution is 1.25° latitude x 1.875° longitude (~200 x 140 km) at the
128 equator with 38 vertical levels extending up to 39 km altitude. The land-based anthropogenic,
129 biomass burning, and shipping emissions are taken from Lamarque et al. (2010), and represent a
130 decadal (1997-2006) mean centered on the year 2000. The use of an emission pattern from 1997-
131 2006 can lead to an overestimation of O_3 concentrations by the model, since the emissions vary on a
132 year to year basis and are expected to be lower in recent years due to the reduction in Amazonian
133 deforestation via burning, consequently reducing the amount of O_3 precursors. HadGEM2 runs at a
134 30-minute time step with the exception of global radiation, which is updated every 3 hours and
135 provides radiative fluxes between those time steps via interpolation. This configuration is described
136 and evaluated in O'Connor et al. (2014) with the exception of the Extended Tropospheric
137 Chemistry (ExtTC) that has been applied in this work. The ExtTC mechanism has been designed to
138 represent the key species and reactions in the troposphere in as much detail as is necessary to
139 simulate atmospheric composition-climate couplings and feedbacks while retaining the capability to

conduct decade-long climate simulations. UKCA-ExtTC simulates the spatial distribution and evolution in time of 89 chemical species, 63 of which are model tracers. The model includes emissions from anthropogenic, biogenic, soil, and wildfire sources for 17 species: nitrogen oxides (NO_x = NO +NO_2), CH_4, carbon monoxide (CO), hydrogen (H_2), methanol, formaldehyde, acetaldehyde and higher aldehydes, acetone, methyl ethyl ketone, ethane (C_2H_6), propane (C_3H_8), butanes and higher alkanes, ethene (C_2H_4), propene (C_3H_6), isoprene, (mono)terpenes, and a lumped species representing aromatics (toluene + xylene) from anthropogenic sources.

Emissions of biogenic species (isoprene, terpenes, methanol, acetone) are computed by iBVOC and provided to UKCA at every time step. The isoprene emission scheme is that of Pacifico et al. (2011). Terpenes, methanol, and acetone emissions are simulated with the model described in Guenther et al. (1995). Anthropogenic and wildfire emissions are prescribed from monthly mean emission data sets prepared for CMIP5 using the historic scenario (Lamarque et al., 2010). Given the difficulty in prescribing a diurnal cycle for fire emissions, these monthly mean emissions are kept constant during the day. Wetland methane emissions are prescribed from data from Gedney et al. (2004). Soil-biogenic NO_x emissions are prescribed using the monthly distributions provided by the Global Emissions Inventory Activity (http://www.geiacenter.org/inventories/present.html), which are based on the global empirical model of soil-biogenic NO_x emissions of Yienger and Levy (1995). NO_x emissions from global lightning activity are parameterized based on the convective cloud top height following Price and Rind (1992, 1994) and are thus sensitive to the model climate. UKCA also includes a dry deposition scheme based on the resistance in-series approach as outlined in Wesely (1989). Physical removal of soluble species is parameterized as a first-order loss process based on convective and stratiform rainfall rates (Collins et al., 2011).

The TRIFFID vegetation module of HadGEM2 simulates the dynamics of five plant functional types (PFTs): broadleaf trees, needleleaf trees, shrubs, and C_3 and C_4 grass (i.e., grasses using the C_3 and C_4 photosynthetic pathway, respectively). Changes in the extent of croplands over time are not simulated but are prescribed from land use maps prepared for the Coupled Model Intercomparison Project 5 (CMIP5, Taylor et al., 2012). Here we use the historic (1850–2000; Hurtt et al., 2009) data sets, as described in Jones et al. (2011). A further four surface types (urban, inland water, bare soil, and ice) are used in the land-surface scheme for the calculation of water and energy exchanges between the land and the atmosphere. Each model grid box can include varying proportions of several vegetation and/or surface types. The model does not include interactive deforestation due to fire.

The parameterization of O_3 damage on vegetation is that of Sitch et al., (2007). This scheme uses a flux-gradient approach to model O_3 damage, rather than empirical approaches based on the accumulated O_3 exposure above 40 ppb (e.g. Felzer, et al. 2005). The Sitch et al. (2007) parameterization assumes a suppression of net leaf photosynthesis by O_3 that varies proportionally to the O_3 flux through stomata above a specified critical O_3 deposition flux. The critical deposition flux depends on O_3 concentration near the leaves, but also on stomatal conductance. This scheme also includes a relationship between stomatal conductance and photosynthesis, determining a reduction in stomatal conductance through O_3 deposition. As the O_3 flux itself depends on the stomatal conductance, which in turn depends upon the net rate of photosynthesis, the model requires a consistent solution for the net photosynthesis, stomatal conductance and the O_3 deposition flux. This approach to modelling O_3 effects on photosynthesis accounts for the complex interaction between CO_2 and O_3 effects, and can be used to study future climate impacts. This scheme includes a 'high' and 'low' parameterization for each PFT to represent species more sensitive and less sensitive to O_3 effects; in our analysis we use the 'high' sensitivity mode to establish the maximum response. The model was calibrated with data from temperate and boreal vegetation. Calibration data for other ecosystems, including tropical vegetation, are currently unavailable.

Description of the model experiments

All simulations use HadGEM2 in its atmosphere-only configuration, i.e., with all implemented couplings between atmosphere and land surface (including carbon cycle) active but without the atmosphere-ocean coupling. HadGEM2 was initialized with equilibrium concentrations of the major chemical components (O_3, CO, H_2, total reactive nitrogen (NO_y), BVOCs) taken from the CMIP5 simulation (see description of the simulations in Jones et al., 2011). Methane mixing ratios were prescribed as specified by CMIP5, with values of 1750 ppb for present-day. The decade-mean CO2 atmospheric mixing ratio was 368 ppm.

Monthly means of sea surface temperature and sea ice cover were prescribed using climatologies derived from the appropriate decade of the Hadley Centre CMIP5 transient climate run Jones et al., (2011). The vegetation distribution for each of our simulations was prescribed using the simulated vegetation averaged for the same decade from this transient climate run, on which we superimposed crop area as given in the CMIP5 historic and future land use maps (Hurtt et al., 2009; Riahi et al., 2007).

We performed a 9-year (2001-2009) control simulation for present-day climate conditions initialized from a centennial transient climate simulation with ocean couplings (Jones et al., 2011). We analysed the last 8 years of the simulation, as the first year of simulation was used as spin-up. A single year is considered sufficient for spin-up because one year is around five times longer than the lifetime of the longest lived atmospheric species (with the exclusion of methane) involved in O_3 chemistry. The control simulation was driven by anthropogenic and wildfire emissions of trace gases and aerosols via historical scenarios (Global Fire Emissions Database GFEDv2; Lamarque et al., 2010; Van der Werf et al., 2006) of anthropogenic and wildfire emissions.

HadGEM2 is able to reproduce the main spatial distribution of surface temperature (Figure S1) and precipitation (Figure S2). Surface temperature simulated with HadGEM2 exhibits a bias in the region of up to 2∞C colder than in the observations over the Amazon forest. Simulated precipitation rate is in reasonable agreement with observations. The model is able to reproduce the main features of the seasonal cycle of precipitation, but tends to simulate less precipitation in September and November than the observations (Figure S03).

Simulated HadGEM2 NPP is compared against a meta-analysis of field data from the Ecosystem Model Data Model Intercomparison project (EMDI) (Olson et al., 2001). Measurements from the 81 'class A' ("well documented and intensively studied") sites, representative of all major global biomes, are compared against our simulations. Traditionally, global vegetation models underestimate NPP in tropical ecosystems, and tend towards an asymptote of ~1000 g C m^{-2} (Prentice et al., 2007). HadGEM2 is able to reproduce the main geographical variations of NPP globally (Figure S4), especially in the Northern Hemisphere, where more plentiful observations are available. In addition HadGEM2 is able to better simulate higher tropical NPP.

Ozone concentration simulated with HadGEM2-UKCA-ExtTC agrees better with observations at higher altitudes and higher latitudes (Figure S5). The model performs more poorly than the ACCENT mean over tropical areas, especially closer to the surface. Comparison with a selection of observed profiles of O_3 concentration shows the model overestimates O_3 for some locations but is in extremely good agreement for others. Over the tropics the agreement is better in the few continental profiles than the marine environment (Figure S6). Some differences may be expected given that the observations are from campaigns with specific meteorological conditions, while the model simulations represent a multi-year mean from the model. Comparison with a selection of surface O_3

observations (Figure S7) confirms again how the model shows a better agreement with observations taken at higher latitudes.

We also perform 10 experiments that differ from the control simulation in terms of assumed biomass burning emissions, i.e. biomass burning emissions over South America are either increased or decreased by +/-20, 40, 60, 80, 100%, while emissions over the rest of the world are kept unchanged. The vegetation distribution was not adjusted for loss of vegetation due to fire. We define biomass burning emissions as those from wildfires, deforestation fires, agricultural forest burning, residential and commercial combustion, including fuel wood burning, charcoal production and biofuel combustion for cooking and heating (Lamarque et al., 2010). The dominant fire types in South America are from deforestation and degradation fires in an arc around Amazonia, with some regional hotspots of agricultural burning (see Figure 13 in Van der Werf et al., 2010). Between 2001 and 2009 the percentage contribution to annual fire emissions from fire types (deforestation and degradation, grassland and savanna, woodland, forest, agriculture) are (59%, 22%, 10%, 8%, 2%) over Southern Hemisphere South America (Figure 13 van der Werf et al., 2010), with minor differences in this region between this dataset (Global Fire Emissions Database GFEFv3) and the earlier GFEDv2 used in this study (see Fig. 16 in Van der Werf et al., 2010). The residential and commercial combustion contribution accounts for 1 and 8% of the total annual biomass burning emissions of CO and NO_x respectively.

This set of experiments allows us to simulate the impact of biomass burning on surface O_3 and vegetation productivity. The control simulation was also used to evaluate surface O_3 mixing ratios against measurements over the Amazon forest.

Model site-level Evaluation

Over the data-sparse Amazonian region, comprehensive spatial data sets of surface O_3 concentration are extremely limited. We evaluated simulated surface O_3 against observations from two sites that have full annual analyses of O_3 concentration: Porto Velho (Brazil; 8.69∞S; 63.87∞W) and site ZF2 in the Cuieiras forest reserve (Brazil; 2.59∞S; 60.21∞W). O_3 mixing ratios were measured with a UV absorption analyser (Thermo 49i, USA). Observations from both sites have an estimated 4% uncertainty, considering zero noise, zero and span drifts reported in the instrument manual, and the frequency of zero and span checks performed along the experiments.

The Porto Velho sampling site is located in a forest reserve about 5 km NE (generally upwind) from the city of Porto Velho. Large land use change and regional biomass burning makes its atmospheric conditions characteristic of those of the Amazon forest with significant human interference (Brito et al., 2014). The whole region of Porto Velho has been subject to land use change since the 1980s. In Porto Velho, the dry season is from June to October and the wet season from November to May. Measurements of surface O_3 mixing ratios were taken from November 2011 to October 2012 in a forest clearance, at 5 m a.g.l..

The Cuieiras forest reserve in Central Amazonia encloses 380 km^2 of pristine tropical rainforest forest. The reserve is located in the central Amazon Basin, 60 km NNW of downtown Manaus and 40 km from the metropolis margins. This site is relatively undisturbed, as no biomass burning occurs in the forest reserve. Here rain showers are frequent with a short dry season from July to October. Measurements were taken at 39 m a.g.l. at the TT34 tower. The forest canopy height near the tower varied between 30 and 35 m, and the site is described in Martin et al. (2010), Rizzo et al. (2013) and Artaxo et al. (2013). Most of the time, the prevailing trade winds blow over 2000 km of the intact tropical forest before reaching the measurement tower. However, the site was also affected by regional transport of pollutants, either from biomass burning or urban sources (Rizzo et al., 2013). Measurements of surface O_3 mixing ratios were taken from April 2010 to June 2012, with the exclusion of a few months due to instrument maintenance.

We compared simulated (averaged over 8 years of simulations) against observed average O_3 diurnal cycles at each site for each available month. The model overestimates observed monthly averaged hourly O_3 mixing ratios at the surface by about 5-15 ppb for all months at the Porto Velho site, but it reproduces the diurnal and seasonal cycle, including those months affected by biomass burning, i.e. August and September, at the Porto Velho site (Figure 1). The model is able to reproduce the diurnal cycle, including magnitude, at the ZF2 site for about 8 months out of 24. The model overestimates surface monthly averaged hourly O_3 mixing ratios by about 5-10 ppb for the rest of months, which are also the months with lower surface O_3 mixing ratios (Figure 2).

Results

Our analysis is focused on the region enclosed in the red rectangle in figure 3, this is a highly vegetated region with homogeneous topography, and it includes the two sites used for the model evaluation (Porto Velho and ZF2 in the Cuieiras forest reserve). This region of analysis is covered by two PFTs in HadGEM2: broadleaf trees, which is the predominant, and C_3 grass (Figure 3).

Surface O_3 mixing ratios simulated with HadGEM2 are higher during the months of August, September and October over the Amazon forest, and in particular over our region of analysis, because of the higher biomass burning emissions in the model during these months. Monthly average surface O_3 mixing ratios in our control simulation peaks at 55-60 ppb in this region (Figure 4), while the average over the region of analysis is peaked at about 30 ppb in August and September, less in October (Figure 5a, black line).

Monthly total Net Primary Productivity (NPP) in our control simulation reaches its minimum during the months of August and September (Figure 5b, black line), at about 300 TgC/month, corresponding to the end of the dry season.

Decreasing biomass burning emissions over South America by -20%, -40%, -60%, -80%, -100% decreases surface O_3 mixing ratios and increases net productivity. Vice versa, increasing biomass burning emissions over South America by +20%, +40%, +60%, +80%, +100% increases surface O_3 mixing ratios over the region of analysis and subsequently reduces net productivity because of O_3 damage on vegetation (Figure 5c).

These sensitivity tests suggest that decreasing biomass burning emission by 100% over South America brings monthly mean surface O_3 mixing ratios averaged over the region of analysis to about the observed 15 ppb for each month (Figure 5a, dark blue line), even during the dry season, with no values over 35 ppb for any grid-cell (Figure 6). Increasing biomass burning emissions by 100% suggests that monthly mean mixing ratios of surface O_3 averaged over the region of analysis reach 40 ppb in August (Figure 5a), with peaks of about 65-70 ppb in some grid-cells (Figure 6a). For both increases and decreases of between 20 and 80% in South American biomass burning the model simulates almost linear changes in surface O_3 mixing ratios (Figure 6, the figure shows increases and reductions by 40, 60 and 100%).

Suppressing biomass burning emissions (i.e. decreasing biomass burning emission by 100%) over South America increases total NPP over the region of analysis by about 15%, to about 350-370 TgC/month, with peak increases of 60% for a few grid-cells, in August and September (Figure 6b):

342 this quantifies the impact of present-day biomass burning on vegetation productivity. When
343 increasing biomass burning emissions over South America by 100%, monthly total NPP over the
344 region of analysis is reduced by about 10%, i.e. to about 250 TgC/month, in August and September
345 (Figure 5b), with peak values of 50-60% reductions for few grid-cells (Figure 6c). For reductions by
346 20 to 80% in South American biomass burning the model varies NPP almost linearly (Figure 5c).
347 However, the increase in South American biomass burning by 20 to 80% determine a very similar
348 decrease in NPP, e.g. between 7 and 10% decrease in August (Figure 5c). Both increasing and
349 reducing South American biomass burning from 20 to 80% increases the number of grid-cells
350 where a significant variation of NPP takes place (Figure 6b). The percentages given above are
351 significant against inter-annual variability in the control simulation, i.e. we only take into account of
352 the variations above one standard deviation in the control simulation. We also exclude from our
353 analysis the grid-cells with low productivity, i.e. where NPP in the control simulation is below 50
354 gC/m^2/month (i.e. we focus on high productivity regions, e.g. forests).
355
356
357 **Discussion and Conclusions**
358
359 The HadGEM2 model overestimates the magnitude of the O_3 diurnal cycle at the two sites used in
360 the evaluation. Overestimation of simulated O_3 in the Amazonian boundary layer has been observed
361 in other modelling studies, especially in clean air conditions (Bela et al., 2014). Nonetheless, our
362 model reproduces the main features of the diurnal and seasonal cycle. In particular, the model is
363 able to reproduce the increase in surface O_3 during the biomass burning season.
364
365 As stated earlier in the model description section, biomass burning emissions are prescribed as
366 monthly mean and kept constant during the day, and this can have an impact on the hourly and day-
367 to-day variation of surface O_3. For example, O_3 production will respond differently if biomass
368 burning emissions occur during the day or at night, affecting simulated surface O_3 mixing ratios.
369 These issues can be improved by modelling fire and biomass burning emissions interactively. The
370 inclusion of an interactive fire model in HadGEM is currently under development.
371
372 The model overestimates surface O_3 mixing ratios by 5-15 ppb for several months at the ZF2 site in
373 the Cuieiras forest reserve and for all available months at the Porto Velho site. The reasons for these
374 systematic biases in surface O_3 mixing ratio are likely manifold. In a complex, highly coupled

375 system such as the HadGEM2 Earth System Model (ESM) it is not always easy to disentangle all
376 processes and attribute model biases to specific components.
377 We attribute the systematic biases in the surface O_3 mixing ratio to the following, most likely
378 reasons:
379 1. Model resolution in both the horizontal and the vertical dimension
380 2. Uncertainties in emissions, both magnitude, seasonality and location
381 3. Uncertainties in the O_3 dry deposition at the surface
382 Other factors such as uncertainties in the chemical mechanism, the photolysis rates, lightning NO_x
383 production over the area and transport of O_3 and precursors will certainly contribute. We will
384 briefly discuss the three most important (in our opinion) factors that contribute to the systematic
385 biases.
386
387 The relatively coarse resolution of a global ESM simulates mixing ratios of trace species (both trace
388 gases and aerosols) that represent averages over large areas. This issue has been discussed
389 previously in the literature, mostly in relation to air quality modelling (see, e.g., Valari and Menut,
390 2008; Tie et al., 2010; Appel et al. 2011; Thompson and Selin, 2012). In our case one grid box
391 equals approximately 30,000 km^2 (i.e., 200x150 km^2 in longitude and latitude). The implicit
392 averaging pertains both to emission and concentration fields; the predominant consequence is a
393 dilution in each grid-cell. Depending on the chemical regime, this can lead to reduced or enhanced
394 net O_3 production. Additionally, HadGEM2-ES has a relatively coarse vertical resolution.
395 HadGEM2-ES has a lowest model layer depth of 40m (global average) and the vertical profile of O_3
396 will undoubtedly show a gradient as the loss mechanism for O_3 is dominated by the surface (e.g.
397 Colbeck and Harrison, 1967). The measurement level may explain part of the model overestimation,
398 since it is well known that O_3 mixing ratios strongly decrease with height due to deposition within
399 the canopy. The lowest layer of the model has a midpoint height 20 metres above the displacement
400 height for the particular gridbox (generally approximated as 2/3 of the average height of the
401 obstacle, in this case the canopy), while measurements were taken at 5 m and 39 m a.g.l.,
402 respectively, at Porto Velho and ZF2 which are located either in or just above canopy level.
403 Rummel et al. (2007) reports a 5-15 ppb O_3 decrease from 52 to 11 m a.g.l. in a forest site in
404 Amazonia. This steep gradient near the surface is due to surface deposition but also due to in-
405 canopy chemical processing (c.f., e.g., Stroud et al., 2005; Gordon et al., 2014). The latter is not
406 represented in HadGEM2-ES.
407

The remote environment of the Amazon forest is dominated by relatively high concentrations of VOC, particularly of biogenic origin, and low concentrations of nitrogen oxides, NO_x. It is a NO_x-limited environment. In such an environment O_3 is destroyed by reactions with BVOC (mainly isoprene and (mono-)terpenes). This destruction is more pronounced the higher the BVOC concentration becomes. Consequently, conditions in the global model are likely to differ from that of a measurement at a specific point such as those we compare to in Figures 1 and 2. It is a known problem in model evaluation.

Another issue related to model resolution, when comparing global models to point-like observations, is the uncertainty in global emission inventories, both with respect to magnitude and location. In particular the latter will result in discrepancies between modelled concentrations of O_3 and its precursors and point-like observations. But the uncertainties in emission magnitude are also substantial and can reach a factor of two or more in case of biogenic VOC (e.g., Guenther et al., 2006; Arneth et al., 2008, 2011; Pacifico et al., 2011, 2012).

Thirdly, and again related to model resolution, is the representation of O_3 dry deposition at the surface. Its magnitude and diurnal cycle will depend on boundary layer turbulence, surface roughness, land surface type, vegetation type, soil moisture, photosynthetic activity, and more. In a recent sensitivity study by Folberth et. al (in preparation) O_3 surface concentrations showed the largest sensitivity to perturbations in O_3 surface dry deposition fluxes. Underestimating O_3 surface dry deposition, in particular during the night preventing a complete flush of the PBL with respect to O_3, will lead to systematic biases.

A comparison with Rummel et al. (2007) indicates that ozone dry deposition velocities on average compare favourably with observations. Rummel at al. (2007) reported day-time velocities of up to 2 cm/s and night-time velocities of typically around 0.5 cm/s during the wet season and velocities between 0.3 cm/s and 1.0 cm/s during day-time and 0.3 cm/s and 0.8 cm/s during the dry season for one site in the Amazon region. HadGEM2-ES predicts annual mean O_3 deposition velocities of 0.5 to 0.6 cm/s (see Figure S8) in fair agreement with the observations. Furthermore, the model is able to capture well the variability between the wet season and the dry season. However, more data are needed to conduct a robust evaluation, but, this admittedly crude comparison is sufficient to demonstrate a basic capability of HadGEM2-ES to reproduce observed ozone deposition velocities in the Amazon region to a reasonable degree.

Interestingly, however, the latter process may also represent a redeeming feature of the model. According to our model of O_3 plant damage it is the total O_3 flux into the plant that determines the amount of damage caused to the photosynthetic activity and, hence, carbon assimilation. However, the total O_3 flux (or dose) is a function of both O_3 surface concentrations and dry deposition, i.e. for plants there is a compensation effect when concentrations are overestimated while deposition velocities are underestimated. Underestimating the O_3 dry deposition flux implies reduced O_3 plant uptake, and consequently an underestimation of the plant damage and productivity losses. However, it also leads to higher O_3 concentrations, which subsequently act to increase plant O_3 uptake and damage, compensating for the initial effects on productivity. Still, a detailed assessment and quantification of this interdependence of O_3 concentration and dry deposition fluxes is beyond the scope of this study and must be referred to future research.

August, September and October are the months when biomass burning and surface O_3 concentrations are higher over the Amazon forest, but also the months when plant productivity is at its lowest which will tend to suppress the impact of O_3 damage on plant productivity. This is because stomatal conductance is reduced due to water limitations (also accounted for in the model) during the dry season, thus reducing the flux of both carbon dioxide and O_3 into the leaves, and consequently reducing O_3 plant damage.

Ashmore (2005) noted how O_3 exposure is poorly correlated with flux into leaves and also the potential for damagingly high O_3 fluxes in leaves at concentrations significantly below 40 ppb at maximum stomatal conductance. Consequently, global vegetation models as used in this study have adopted flux-based parameterizations to represent O_3 impacts on vegetation, moving away from application of the earlier exposure based metrics, e.g. accumulated O_3 exposure above a threshold of 40 ppb, AOT40.

The parameterization of O_3 damage used in this study is calibrated for high-latitude vegetation. Unfortunately data for calibrating this O_3 damage scheme for tropical vegetation are currently not available and observations of O_3 damage in the Amazon forest are very limited. Observations of O_3 damage on tropical forests are urgently needed, including observations at moderate (e.g. 20-30 ppb) and high surface O_3 mixing ratios.

The simulated impact of present-day biomass burning on vegetation productivity over our area of analysis is about 230 TgC/yr (i.e. the difference between the dark blue line and the black line in Fig.

5b) using the "high" sensitivity mode in the O_3 damage scheme. Taking into account that the uncertainty in these estimates is substantial, this O_3 damage impact over the Amazon forest is of the same order of magnitude as the release of CO_2 due to land fire in South America, as quantified in van der Werf et al., (2010; 293 TgC/yr from table 7 of that paper); in effect to potentially double the impact of biomass burning on the CO_2 fluxes. This highlights the urgent need for more tropical data on plant O_3 damage to better constrain estimates.

Despite overestimating surface O_3 mixing ratios our model simulates only a moderate reduction in NPP associated with elevated O_3 due to biomass burning emissions. Given that our model systematically overestimates O_3 mixing ratio, assuming accurate dry deposition, and that we use our model in the high sensitivity mode, our simulations where we increase biomass burning emissions by 100% suggest a maximum 10% average reduction in monthly plant productivity, and peak reductions of 50-60% reductions in few grid-cells. This is because, despite the increase in biomass burning, monthly average surface O_3 mixing ratios do not exceed a moderate 40 ppb. Moreover, our model does not include deforestation due to fire, which would reduce vegetation cover when increasing biomass burning emissions in our sensitivity experiments, reducing NPP, and BVOC emissions, further. However, local and daily/hourly impact of O_3 damage on plant productivity can be higher.

Estimates of the magnitude of the reduction in plant productivity due to O_3 damage can be improved with additional field studies and improving the representation of tropospheric O_3 in ESMs (sources, chemistry and sinks). Nevertheless, considering these processes in a coupled system can provide an improvement in robustness of conclusions, as e.g. it can treat processes with a specific diurnal cycle, like photosynthesis and surface O_3, interactively on a short time scale (e.g. half an hour in our model).

Acknowledgments

This work was funded by the Natural Environment Research Council (NERC) South AMerican Biomass Burning Analysis (SAMBBA) project grant code NE/J010057/1. The UK Met Office contribution to this project was funded by the DECC under the Hadley Centre Climate Programme contract (GA01101). The Brazilian contribution was funded by Fundacao de Amparo a Pesquisa do Estado de Sao Paulo (FAPESP, projects 08/58100-2 and 12/14437-9). We thank INPA (Instituto Nacional de Pesquisas da Amazonia) for the coordination work of the LBA Experiment. We thank USP technicians for the support on data sampling: Alcides Ribeiro, Ana Lucia Loureiro, Fernando Morais and Fabio Jorge.

References

Ainsworth, E. A., Yendrek, C. R., Sitch, S., Collins, W. J. and Emberson, L. D.: The Effects of Tropospheric Ozone on Net Primary Productivity and Implications for Climate Change, Annu. Rev. Plant Biol., 63, 637-61, 2012.

Appel, K. W., Foley, K. M., Bash, J. O., Pinder, R. W., Dennis, R. L., Allen, D. J. and Pickering, K.: A multi-resolution assessment of the Community Multiscale Air Quality (CMAQ) model v4.7 wet deposition estimates for 2002-2006, Geosci. Model Dev., 4, 357-371, 2011.

Arneth, A., Monson, R. K., Schuregers, G., Niinemets, Ü. and Palmer, P. I.: Why are estimates of global terrestrial isoprene emissions so similar (and why is it not so for monoterpenes), Atmos. Chem. Phys., 8, 4605-4620, 2008.

Arneth, A., Schurgers, G., Lathiere, J., Duhl, T., Beerling, D. J., Hewitt, N., Guenther, A.: Global terrestrial isoprene emission in models: sensitivity to variability in climate and vegetation, Atmos. Chem. Phys., 11, 8037-8052, 2011.

Artaxo, P., Martins, J. V., Yamasoe, M. A., Procópio, A. S., Pauliquevis, T. M., Andreae, M. O., Guyon, P., Gatti, L. V., Leal., A. M. C.: Physical and chemical properties of aerosols in the wet and dry season in Rondônia, Amazonia. J. Geophys. Res., 107, D20, 8081-8095, 2002.

Artaxo, P., Gatti, L V., Leal, A. M. C, Longo, K. M., de Freitas, S. R., Lara, L. L., Pauliquevis, T. M., Procópio, A. S., Rizzo, L. V.: Atmospheric Chemistry in Amazonia: The forest and the biomass burning emissions controlling the composition of the Amazonian atmosphere, Acta Amazonica, 35(2), 185-196, 2005.

Artaxo, P., Rizzo, L. V., Brito, J. F., Barbosa, H. M. J., Arana, A., Sena, E. T., Cirino, G. G., Bastos, W., Martin, S. T., Andreae. M. O.: Atmospheric aerosols in Amazonia and land use change: from natural biogenic to biomass burning conditions. Faraday Discussions, 2013

Ashmore, M. R: Assessing the future global impacts of ozone on vegetation, Plant Cell Environ., 28, 949-964, 2005.

546

547 Bela, M. M., Longo, K. M., Freitas, S. R., Moreira, D. S., Beck, V., Wofsy, S. C., Gerbig, C.,
548 Wiedemann, K., Andreae, M. O., and Artaxo, P.: Ozone production and transport over the Amazon
549 Basin during the dry-to-wet and wet-to-dry transition seasons, Atmos. Chem. Phys. Discuss., 14,
550 14005–14070, 2014

551

552 Brito, J., Rizzo, L. V., Morgan, W. T., Coe, H., Johnson, B., Haywood, J., Longo, K., Freitas, S.,
553 Andreae, M. O. and Artaxo, P.: Ground based aerosol characterization during the South American
554 Biomass Burning Analysis (SAMBBA) field experiment, Atmos. Chem. Phys. Discuss., 14, 12279-
555 12322, 2014.

556

557 Burnett, R. T., Brook, J. R., Yung, W. T., Dales, R. E., Krewski, D.: Association between Ozone
558 and Hospitalization for Respiratory Diseases in 16 Canadian Cities, Environ. Res., 72, 1, 24-31,
559 1997.

560

561 Cirino, G.G., Souza, R. F., Adams, D. K. and Artaxo, P.: The effect of atmospheric aerosol particles
562 and clouds on net ecosystem exchange in Amazonia, Atmos. Chem. Phys. Discuss., 13,
563 28819–28868, 2013.

564

565 Clark, D. B., Mercado, L. M., Sitch, S., Jones, C. D., Gedney, N., Best, M. J., Pryor, M., Rooney,
566 G. G., Essery, R. L. H., Blyth, E., Boucher, O., Harding, R. J., Huntingford, C. and Cox, P. M.: The
567 Joint UK Land Environment Simulator (JULES), model description – Part 2: Carbon fluxes and
568 vegetation dynamics, Geosci. Model Dev., 4, 701-722, 2011.

569

570 Colbeck, I. and Harrison, R. M.: Dry deposition of ozone: some measurements of deposition
571 velocity and of vertical profiles to 100 metres, Atm. Environ., 19, 11, 1807-1818, 1967

572

573 Collins, W. J., Bellouin, N., Doutriaux-Boucher, M., Gedney, N., Halloran, P., Hinton, T., Hughes,
574 J., Jones, C. D., Joshi, M., Liddicoat, S., Martin, G., O'Connor, F., Rae, J., Senior, C., Sitch, S.,
575 Totterdell, I., Wiltshire, A. and Woodward, S.: Development and evaluation of an Earth-system
576 model-HadGEM2, Geosci. Model Dev., 4, 1051–1075, 2011.

577

578 Cox, P. M., Huntingford, C. and Harding, R. J.: A canopy conductance and photosynthesis model
579 for use in a GCM land surface scheme, J. Hydrol., 212–213, 79–94, 1998._

Cox, P. M., Betts, R. A., Bunton, C. B., Essery, R. L. H., Rowntree, P. R. and Smith, J.: The impact of new land surface physics on the GCM simulation of climate and climate sensitivity, Clim. Dyn., 15, 183–203, 1999.

Cox, P. M.: Description of the "TRIFFID" Dynamic Global Vegetation Model, Tech. Note 24, 17 pp., Met Off. Hadley Cent., Exeter, U. K, 2001.

Emmons, L., Hauglustaine, D., Muller, J., Carroll, M., Brasseur, G., Brunner, D., Staehelin, J., Thouret, V., and Marenco, A.: Data composites of airborne observations of tropospheric ozone and its precursors, J. Geophys. Res., 105, 20497–20538, 2000.

Essery, R. L. H., Best, M. J., Betts, R. A., Cox, P. M. and Taylor, C. M.: Explicit representation of subgrid heterogeneity in a GCM Land Surface Scheme, J. Hydrometeorol., 4, 530–543, 2003.

Felzer, B., Reilly, J., Melillo, J., Kicklighter, D., Sarofim, M., Wang, C., Prinn, R. and Zhuang, Q.: Future effects of ozone on carbon sequestration and climate change policy using a global biogeochemical model, Clim. Change 73, 345–373, 2005.

Felzer, B. S., Cronin, T., Reilly, J. M., Melillo, J. M. and Wang, X.: Impacts of ozone on trees and crops, C. R. Geosci., 339, 784–798, 2007.

Fiscus, E. L., Booker, F. L., Burkey, K. O.: Crop responses to ozone: uptake, modes of action, carbon assimilation and partitioning, Plant Cell Environ, 28, 997-1011, 2005.

Fishman et al., 1996 Fishman, J., Hoell, J., Bendura, R., McNeil, R., and Kirchhoff, V.: NASA GTE TRACE A experiment (September October 1992): Overview, J. Geophys. Res., 101, 23865–23879, doi:10.1029/96JD00123, 1996.

Folberth, G. A., Abraham, N. L., Dalvi, M., Johnson, C. E., Morgenstern, O., O'Connor, F. M., Pacifico, F., Young, P. A., Collins, W. J., and Pyle, J. A.: Evaluation of the new UKCA climate-composition model. Part IV. Extension to Tropospheric Chemistry and Biogeochemical Coupling between Atmosphere and Biosphere, Geosci. Model Dev. (in preparation)

614 Gatti et al.: Drought sensitivity of Amazonian carbon balance revealed by atmospheric
615 measurements, Nature 506, 76-80, 2014.
616
617 Gedney, N., Cox, P. M. and Huntingford, C.: Climate feedback from wetland methane emissions,
618 Geophys. Res. Lett., 31, L20503, 2004.
619
620 Gordon, M., Vlasenko, A., Staebler, R. M., Stroud, C., Makar, P. A., Liggio, J., Li, S.-M., and
621 Brown, S.: Uptake and emission of VOCs near ground level below a mixed forest at Borden,
622 Ontario, Atmos. Chem. Phys., 14, 9087–9097, 2014.
623
624 Grace, J., Mahli, Y., Higuchi, N., Meir, P.,: Productivity and carbon fluxes of tropical rain forest.
625 In: J.Roy, H.A.M. (Ed). Global Terrestrial Productivity. Academic Press, San Diego, 2001.
626
627 Guenther, A., Hewitt, C. N., Erickson, D., Fall, R., Geron, C., Graedel, T., Harley, P., Klinger, L.,
628 Lerdau, M., Mckay, W. A., Pierce, T., Scholes, B., Steinbrecher, R., Tallamraju, R., Taylor, J., and
629 Zimmerman, P.: A global model of natural volatile organic compound emissions, J. Geophys. Res.,
630 100(D5), 8873– 8892, 1995.
631
632 Guenther, A., Karl, T., Harley, P., Wiedinmyer, C., Palmer, P. I. and Geron, C.: Estimates of global
633 terrestrial isoprene emissions using MEGAN (Model of Emissions of Gases and Aerosols from
634 Nature), Atmos. Chem. Phys., 6, 3181-321-, 2006.
635
636 Harris, I., Jones, P. D., Osborn, T. J., Lister, D. H.: Updated high-resolution grids of monthly
637 climatic observations – the CRU TS3.10 Dataset, Int. J. Climatol., 34, 632-642, 2014.
638
639 Hurtt, G. C., et al.: Harmonization of global land-use scenarios for the period 1500–2100 for IPCC-
640 AR5, iLEAPS Newsl., 7, 6–8, 2009.
641
642 Jones, C. D., et al.: The HadGEM2-ES implementation of CMIP5 centennial simulations, Geosci.
643 Model Dev. Discuss., 4(1), 689–763, 2011.
644
645 Karl, T., Yokelson, R., Guenther, A., Greenberg, J., Blake, D., Artaxo, P.: TROFFEE (TROpical
646 Forest and Fire Emissions Experiment): Investigating Emission, Chemistry, and Transport of
647 Biogenic Volatile Organic Compounds in the Lower Atmosphere over Amazonia. J. Geophys. Res.,

112, (D18), D18302, 2007.

Kirkman, G. A., Gut, A., Ammann, C., Gatti, L. V, Cordova, A. M., Moura, M. A. L., Meixner, F. X.: Surface exchange of nitric oxide, nitrogen dioxide, and ozone at a cattle pasture in Rondônia, Brazil, J. Geophys. Res., 107(D20), 8083, 2002.

Kvalevag M. M., Myhre, G.: The effect of carbon-nitrogen coupling on the reduced land carbon sink caused by tropospheric ozone, Geophys. Res. Letters, 40, 1-5, 2013.

Lamarque, J.-F., et al.: Historical (1850–2000) gridded anthropogenic and biomass burning emissions of reactive gases and aerosols: Methodology and application, Atmos. Chem. Phys., 10, 7017–7039, 2010.

Le Quéré, C. M. R., Raupach, J. G., Canadell, G. Marland et al.: Trends in the sources and sinks of carbon dioxide, Nature Geosciences, 2, 2009.

Lippmann, M.: Health effects of tropospheric ozone: review of recent research findings and their implications to ambient air quality standards, J. Exp. An. Environ. Epid., 3(1), 103-129, 1993.

Lloyd. J., Kolle, O., Fritsch, H., de Freitas, S. R., Dias, M. A. F. Silva, Artaxo, P., Nobre, A. D., de Araujo, A. C., Kruijt, B., Sogacheva, L., Fisch, G., Thielmann, A., Kuhn, U., Andreae, M. O.: An airborne regional carbon balance for Central Amazonia, Biogeosciences 4 (5): 759-768, 2007.

Logan, J., Megretskaia, I., Miller, A., Tiao, G., Choi, D., Zhang, L., Stolarski, R., Labow, G., Hollandsworth, S., Bodeker, G., Claude, H., De Muer, D., Kerr, J., Tarasick, D., Oltmans, S., Johnson, B., Schmidlin, F., Staehelin, J., Viatte, P., and Uchino, O.: Trends in the vertical distribution of ozone: A comparison of two analyses of ozonesonde data, J. Geophys. Res., 104, 26373–26399, doi:10.1029/1999JD900300, 1999.

Martin, S. T., Andreae, M. O., Althausen, D., Artaxo, P., Baars, H., Borrmann, S., Chen, Q., Farmer, D. K., Guenther, A., Gunthe, S. S., Jimenez, J. L., Karl, T., Longo, K., Manzi, A., Müller, T., Pauliquevis, T., Petters, M. D., Prenni, A. J., Pöschl, U., Rizzo, L. V., Schneider, J., Smith, J. N., Swietlicki, E., Tota, J., Wang, J., Wiedensohler, A., and Zorn, S. R.: An overview of the Amazonian Aerosol Characterization Experiment 2008 (AMAZE- 08), Atmos. Chem. Phys., 10,

11415-11438, 2010.

Martin, G. M., et al.: The HadGEM2 family of Met Office Unified Model Climate configurations, Geosci. Model Dev., 4, 723–757, 2011.

O'Connor, F. M., Johnson, C. E., Morgenstern, O., Abraham, N. L., Braesicke, P., Dalvi, M., Folberth, G. A., Sanderson, M. G., Telford, A. Voulgarakis, P. J., Young, P. J., Zeng, G., Collins, W. J. and Pyle, J. A.: Evaluation of the new UKCA climate-composition model – Part 2: The Troposphere, Geosci. Model Dev., 7, 41-91, 2014.

Oliveira, P. H. F., Artaxo, P., Pires Jr, C., de Lucca, S., Procópio, A., Holben, B., Schafer, J., Cardoso, L. F., Wofsy, S. C., Rocha, H. R.: The effects of biomass burning aerosols and clouds on the CO_2 flux in Amazonia, Tellus Series B-Chemical and Physical Meteorology, 59B, (3) 338–349, 2007.

Olson, R. J., Scurlock, J. M. O., Prince, S. D., Zheng, D. L. and Johnson, K. R. (eds.). 2001. NPP Multi-Biome: NPP and Driver Data for Ecosystem Model-Data Intercomparison

Ometto, J. P., Nobre, A. D., Rocha, H., Artaxo, P., Martinelli, L.: Amazônia and the Modern Carbon Cycle: Lessons Learned. Oecologia, 143, 4, 483-500, 2005.

Pacifico, F., et al.: Evaluation of a photosynthesis-based biogenic isoprene emission scheme in JULES and simulation of isoprene emissions under present-day climate conditions, Atmos. Chem. Phys., 11, 4371–4389, 2011.

Pacifico, F., Folberth, G. A., Jones, C. D., Harrison, S. P. and Collins, W. J.: Sensitivity of biogenic isoprene emissions to past, present, and future environmental conditions and implications_for atmospheric chemistry, J. Geophys. Res., 117, D22302, 2012.

Palmer, J. R., and Totterdell, I. J.: Production and export in a Global Ocean Ecosystem Model, Deep Sea Res., Part I, 48, 1169–1198, 2001.

Prentice, I. C. , Bondeau A., Cramer W., et al . 2007. Dynamic global vegetation modeling: quantifying terrestrial ecosystem responses to large-scale environmental change. In: Canadell JG,

716 Pataki DE, Pitelka LF, eds. Terrestrial ecosystems in a changing world. IGBP Series. Berlin:
717 Springer, 175 – 192.
718
719 Price, C., and Rind, D.: A simple lightning parameterization for calculating global lightning
720 distributions, J. Geophys. Res., 97, 9919-9933, 1992.
721
722 Price, C., and Rind, D.: Modeling global lightning distributions in a general circulation model,
723 Mon. Weather Rev., 122, 1994.
724
725 Riahi, K., Gruebler, A. and Nakicenovic, N.: Scenarios of long-term socio-economic and
726 environmental development under climate stabilization, Technol. Forecast. Soc. Change, 74(7),
727 887–935, 2007.
728
729 Rich, S.: Ozone damage to plants, Ann. Rev. Phytopathol., 2, 253-266, 1964.
730
731 Rizzo, L. V., Artaxo, P., Muller, T., Wiedensohler, A., Paixao, M., Cirino, G. G., Arana, A.,
732 Swietlicki, E., Roldin, P., Fors, E. O., Wiedemann, K. T., Leal, L. S. M. and Kulmala, M.: Long
733 term measurements of aerosol optical properties at a primary forest site in Amazonia, Atmos.
734 Chem. Phys., 13, 2391–2413, 2013.
735
736 Rummel, U., Ammann, C., Kirkman, G. A., Moura, M. A. L., Foken, T., Andreae, M. O., and
737 Meixner, F. X.: Seasonal variation of ozone deposition to a tropical rain forest in southwest
738 Amazonia, Atmos. Chem. Phys., 7, 5415–5435, 2007.
739
740 Seinfeld, J. H., Pandis, S. N.,: Atmospheric Chemistry and Physics: from Air Pollution to Climate
741 Change. J. Wiley, New York, 1998.
742
743 Sierra, C. A., Harmon, M. E., Moreno, F. H., Orrego, S. A., Del Valle, J. I.: Spatial and temporal
744 variability of net ecosystem production in a tropical forest: testing the hypothesis of a significant
745 carbon sink. Glob. Change Biol., 13, 838–853, 2007.
746
747 Sigler, J. M., Fuentes, J. D., Heitz, R. C., Garstang, M., and Fisch, G.: Ozone dynamics and
748 deposition processes at a deforested site in the Amazon basin, Ambio, 31(1), 21-7, 2002.
749

750 Sitch, S., Cox, P. M., Collins, W. J., Huntingford, C.,: Indirect radiative forcing of climate change
751 through ozone effects on the land-carbon sink, Nature, 448, 791-95, 2007.
752
753 Stroud, C., Makar, P., Karl, T., Guenther, A., Geron, C., Turnipseed, A., Nemitz, E., Baker, B.,
754 Potosnak, M., and Fuentes, J. D., Role of canopy-scale photochemistry in modifying biogenic-
755 atmosphere exchange of reactive terpene species: Results from the CELTIC field study, J. Geophys.
756 Res., 110(D17303), doi:10.1029/2005JD005775, 2005.
757
758 Taylor, J. A., Lloyd, J.: Sources and sinks of atmospheric CO_2. Australian Journal of Botany, 40, 4-
759 5, 407-418, 1992.
760
761 Taylor, K. E., Stouffer, R., J. and Meehl, G. A.: An Overview of CMIP5 and the Experiment
762 Design, B. Am. Meteorol. Soc., 93.4, 2012.
763
764 Thompson et al. (2003a, b) Thompson, A., Witte, J., McPeters, R., Oltmans, S., Schmidlin, F.,
765 Logan, J., Fujiwara, M., Kirchhoff, V., Posny, F., Coetzee, G., Hoegger, B., Kawakami, S., Ogawa,
766 T., Johnson, B., Vomel, H., and Labow, G.: Southern Hemisphere Additional Ozonesondes
767 (SHADOZ) 1998–2000 tropical ozone climatology – 1. Comparison with Total Ozone Mapping
768 Spectrometer (TOMS) and ground-based measurements, J. Geophys. Res., 108, 8238,
769 doi:10.1029/2001JD000967, D2, 2003a.
770
771 Thompson, A., Witte, J., Oltmans, S., Schmidlin, F., Logan, J., Fujiwara, M., Kirchhoff, V., Posny,
772 F., Coetzee, G., Hoegger, B., Kawakami, S., Ogawa, T., Fortuin, J., and Kelder, H.: Southern
773 Hemisphere Additional Ozonesondes (SHADOZ) 1998–2000 tropical ozone climatology – 2.
774 Tropospheric variability and the zonal wave-one, J. Geophys. Res., 108, 8241,
775 doi:10.1029/2002JD002241, D2, 2003b.
776
777 Thompson, T. M., and Selin. N. E.: Influence of air quality model resolution on uncertainty
778 associated with health impacts, Atmos. Chem. Phys., 12, 9753-9762, 2012.
779
780 Tie, X., Brasseur, G. and Ying, Z.: Impact of model resolution on chemical ozone formation in
781 Mexico City: application of the WRF-Chem model, Atmos. Chem. Phys., 10, 8983-8995, 2010.
782
783 van der Werf, G. R., Randerson, J. T., Giglio, L., Collatz, G. J., Kasibhatla, P. S., and Arellano, A.

F.: Interannual variability in global biomass burning emissions from 1997 to 2004, Atmos. Chem. Phys., 6, 3423–3441, 2006.

van der Werf et al.: Global fire emissions and the contribution of deforestation, savanna, forest, agricultural, and peat fires (1997–2009), Atmos. Chem. Phys., 10, 11707–11735, 2010.

Valari, M., and Menut, L.: Does an increase in air quality Models' resolution bring surface ozone concentrations closer to reality?, J. Atm. Oceanic Tech., 25, 2008.

Wesely, M. L.: Parameterization of surface resistances to gaseous dry deposition in regional-scale numerical models, Atmos. Environ., 23, 1293–1304, 1989.

Yienger, J. J., and Levy II, H.: Global inventory of soil-biogenic NOx emissions, J. Geophys. Res., 100, 11,447–11,464, 1995.

798
799 Figures
800
801 1. Comparison of measured (dots) and simulated (stars) monthly averaged diurnal cycle of
802 surface O_3 mixing ratios at the Porto Velho site, including measured day-to-day variability (grey
803 lines) and standard deviation (dashed lines) for the model results. The measurements have an
804 uncertainty of 4%.
805
806 2. Comparison of measured (dots) and simulated (stars) monthly averaged diurnal cycle of
807 surface O_3 mixing ratios at the ZF2 site in the Cuieiras forest reserve, including measured day-to-
808 day variability (grey lines) and standard deviation (dashed lines) for the model results. The
809 measurements have an uncertainty of 4%. We show one of the two available years of observations.
810 Legend as in Figure 1.
811
812 3. Vegetation cover in HadGEM2 for the month of September. The red rectangle is our region
813 of analysis. The two sites used in the model evaluation (the sites of Porto Velho and ZF2 site in the
814 Cuieiras forest reserve) are also marked.
815
816 4. Monthly average surface O_3 mixing ratio simulated with HadGEM2 for the month of
817 September (average over 8 years of simulations).
818
819 5. Clockwise from the top-left: (a) Simulated monthly surface O_3 mixing ratios; (b) Simulated
820 monthly total NPP; (c) Simulated monthly variation in total NPP. The plots show the results for the
821 control simulation (i.e. using the decadal mean biomass burning emissions from Lamarque et al.
822 (2010) centered on year 2000; 2000 BB emissions) and the various experiments with increased (+)
823 or decreased (-) biomass burning emissions over South America by 20, 40, 60, 80 and 100%. All
824 data are averaged over the region of analysis for 8 years of simulations.
825
826 6. From the left: simulated variation in surface O_3 mixing ratios and NPP over the region of
827 analysis for the months of August, September and October.
828
829 7. Probability density function (histogram) of the variation in NPP for the same months. The
830 plots show the variation between the experiments with South American biomass burning
831 increased/decreased by 40, 60 and 100% and the control simulation.

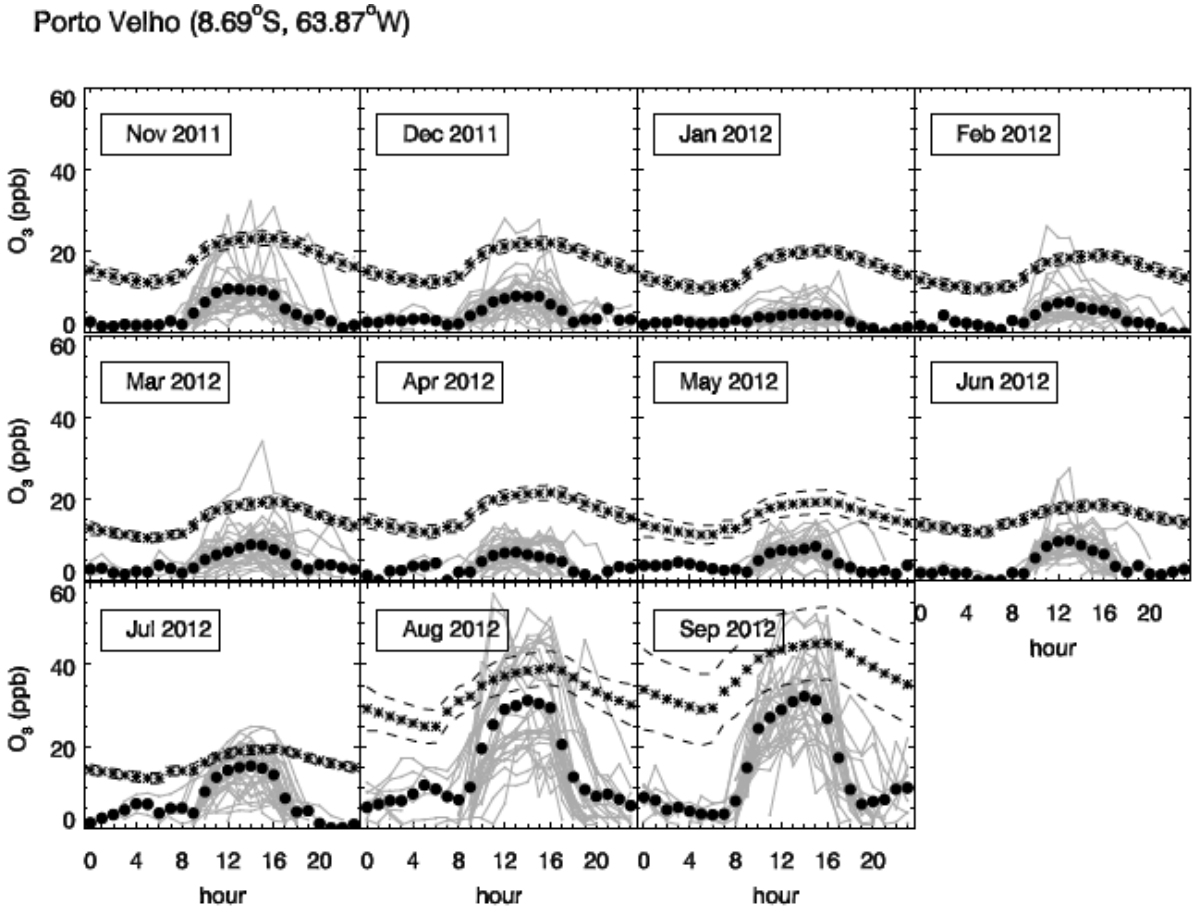

832
833 Figure 1

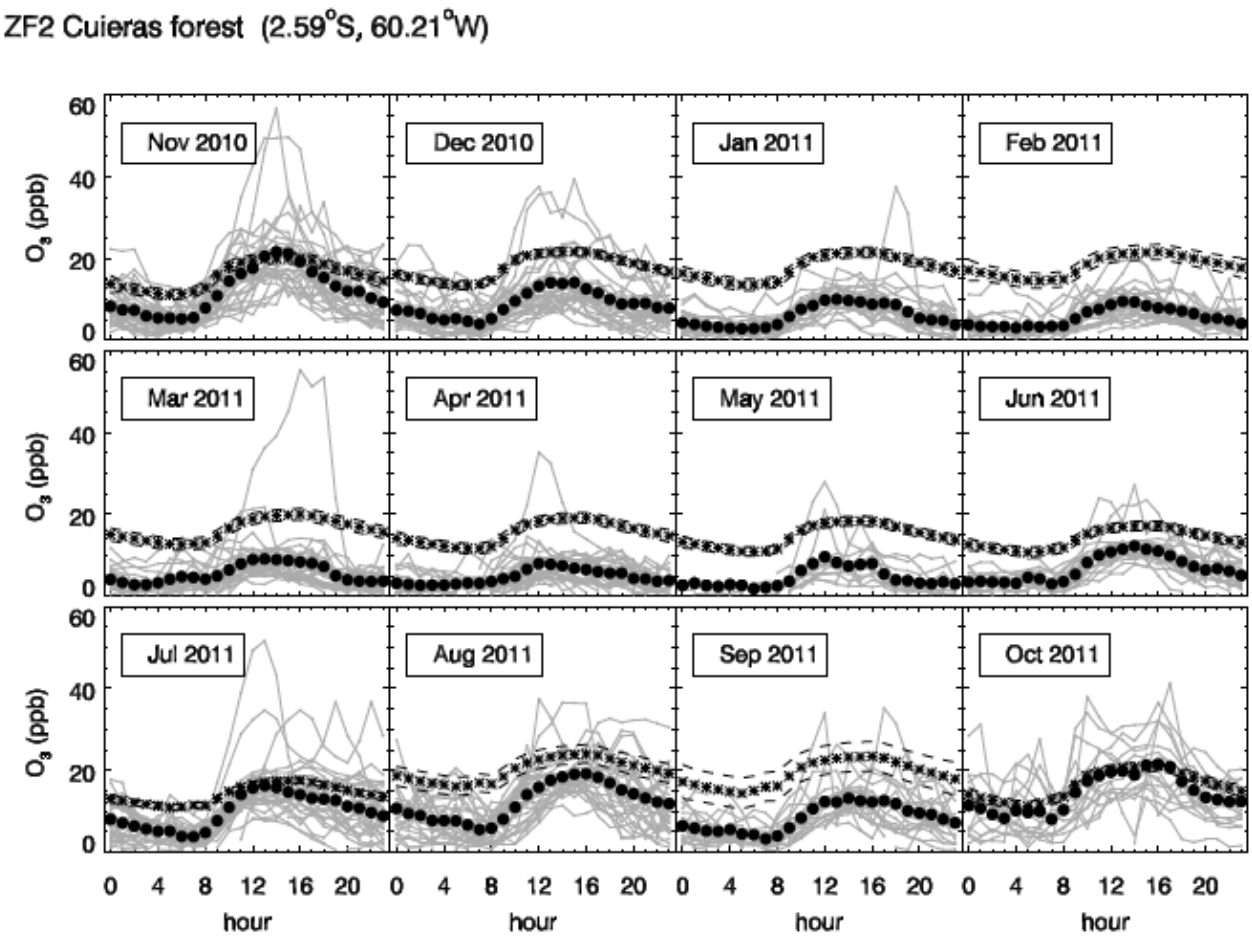

834
835 Figure 2

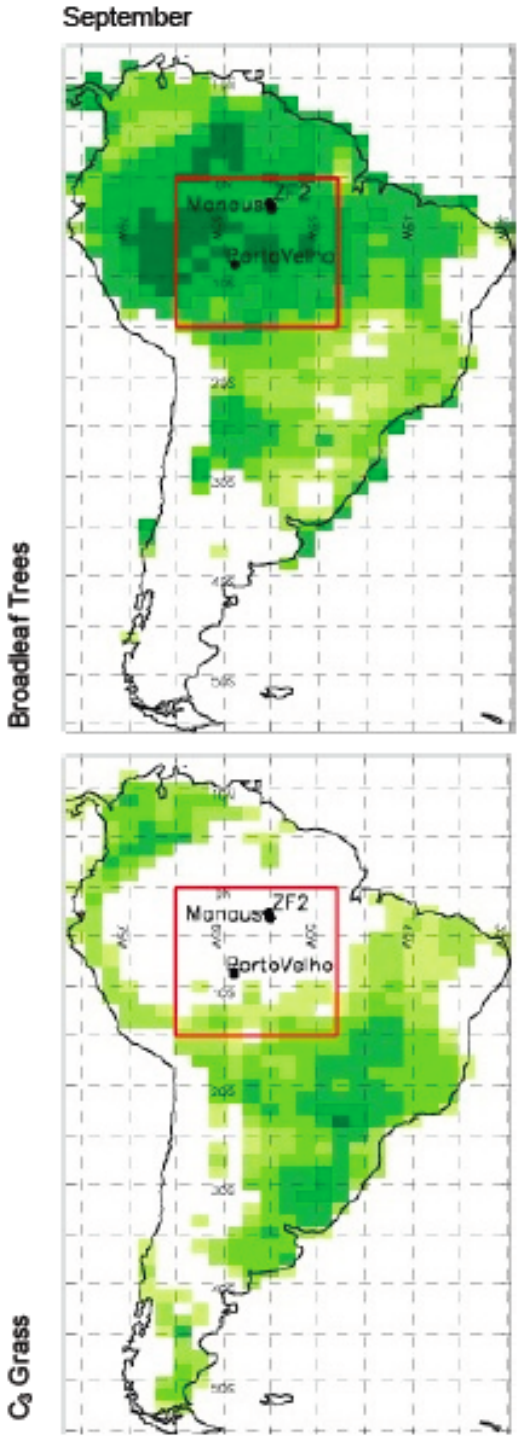

836
837 Figure 3

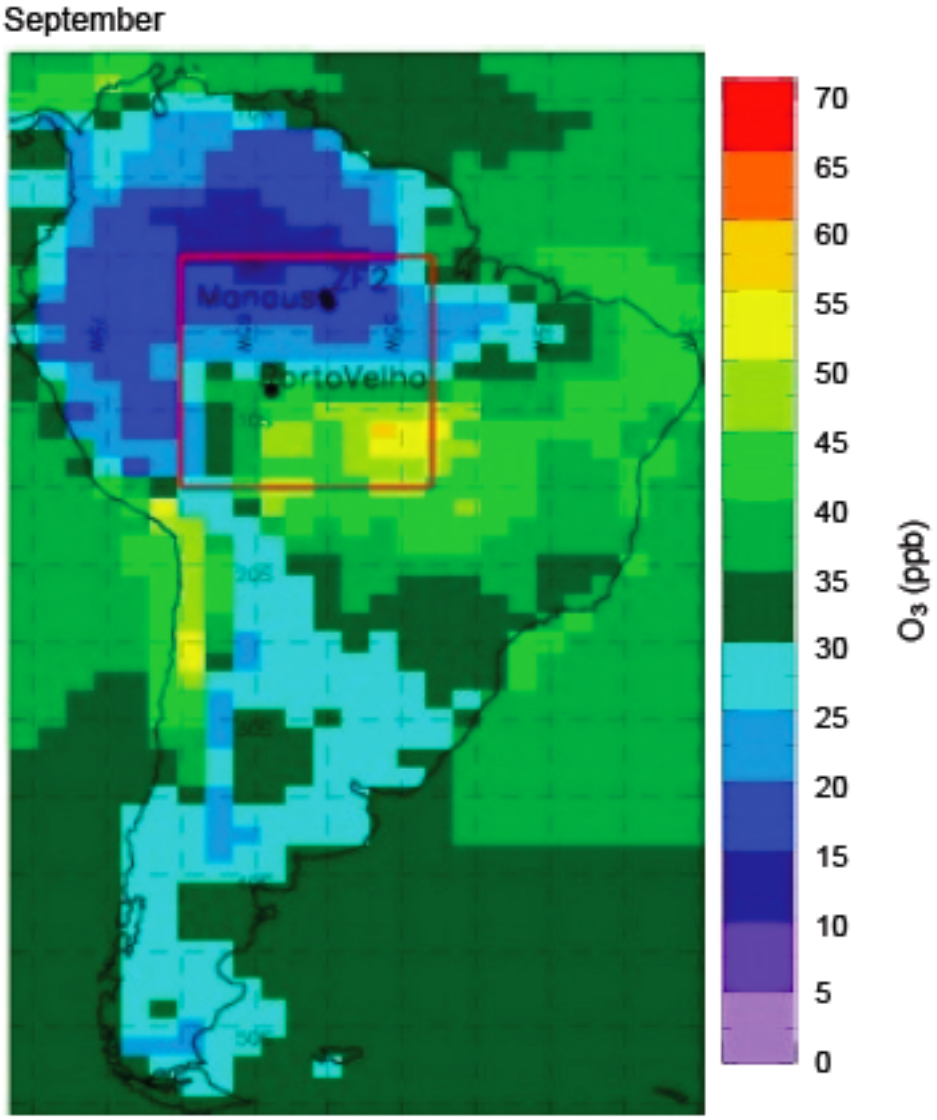

838
839 Figure 4

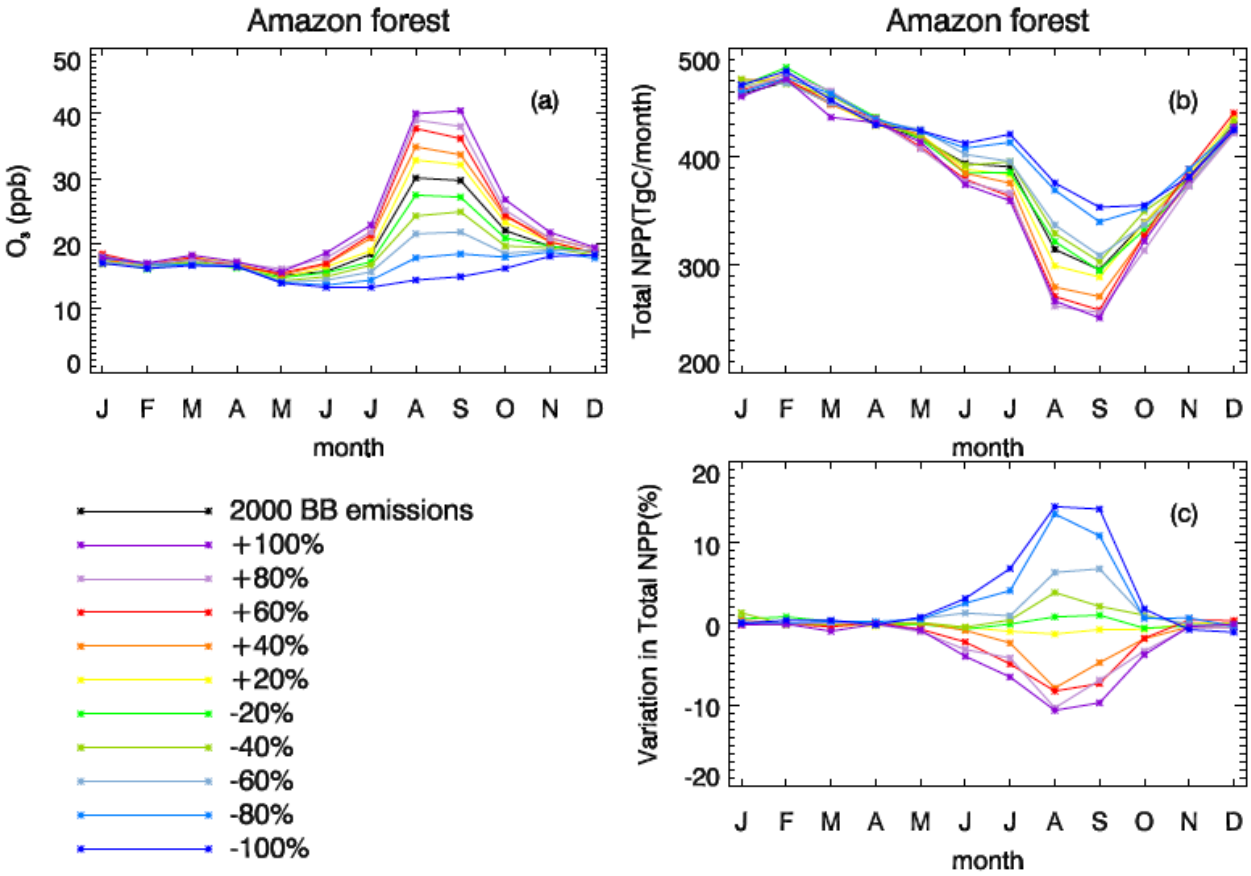
Amazon forest
(a)
O_3 (ppb)
50
40
30
20
10
0
J F M A M J J A S O N D
month
2000 BB emissions
+100%
+80%
+60%
+40%
+20%
-20%
-40%
-60%
-80%
-100%
Amazon forest
(b)
Total NPP(TgC/month)
500
400
300
200
J F M A M J J A S O N D
month
(c)
Variation in Total NPP(%)
20
10
0
-10
-20
J F M A M J J A S O N D
month

Figure 5

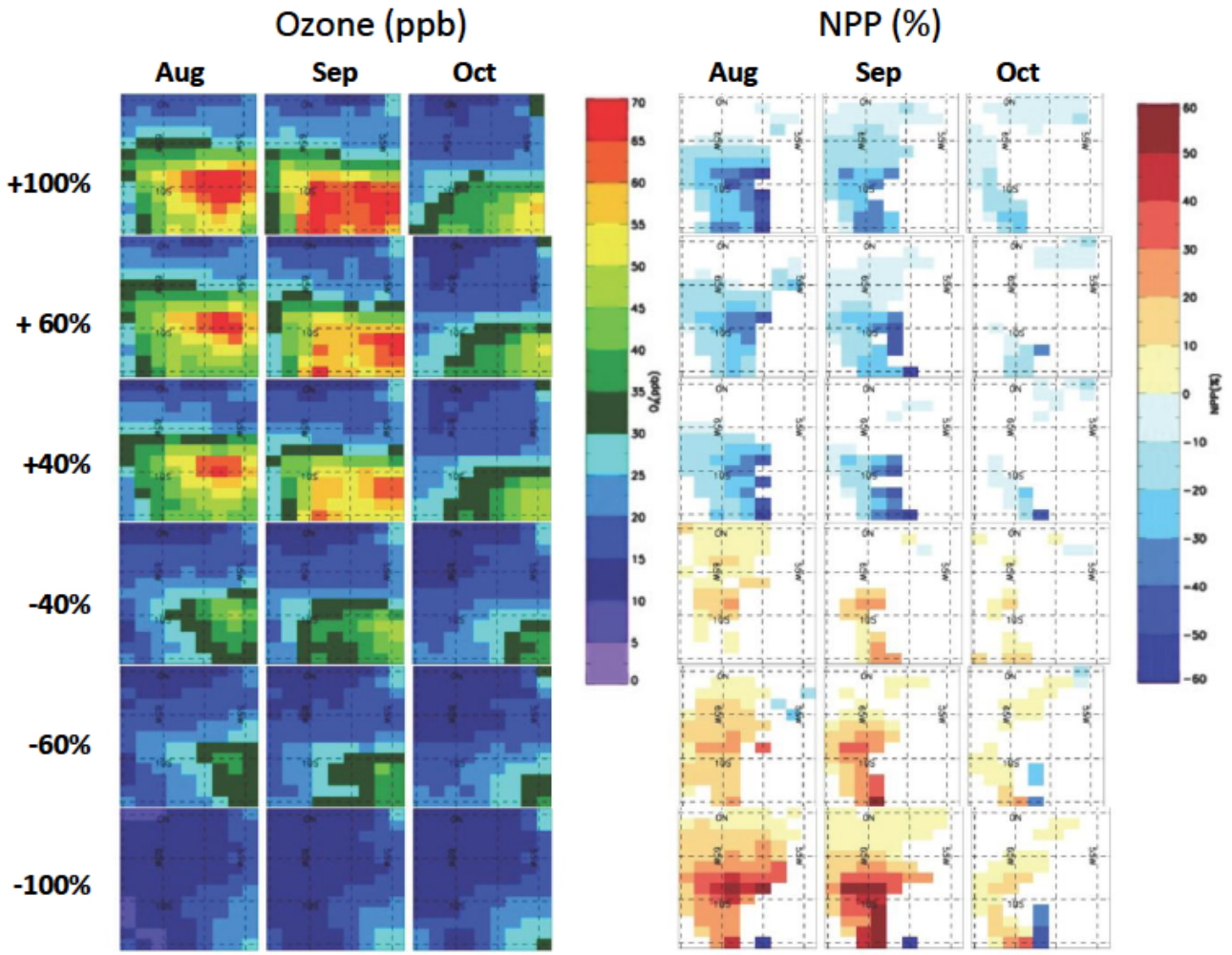

842
843 Figure 6

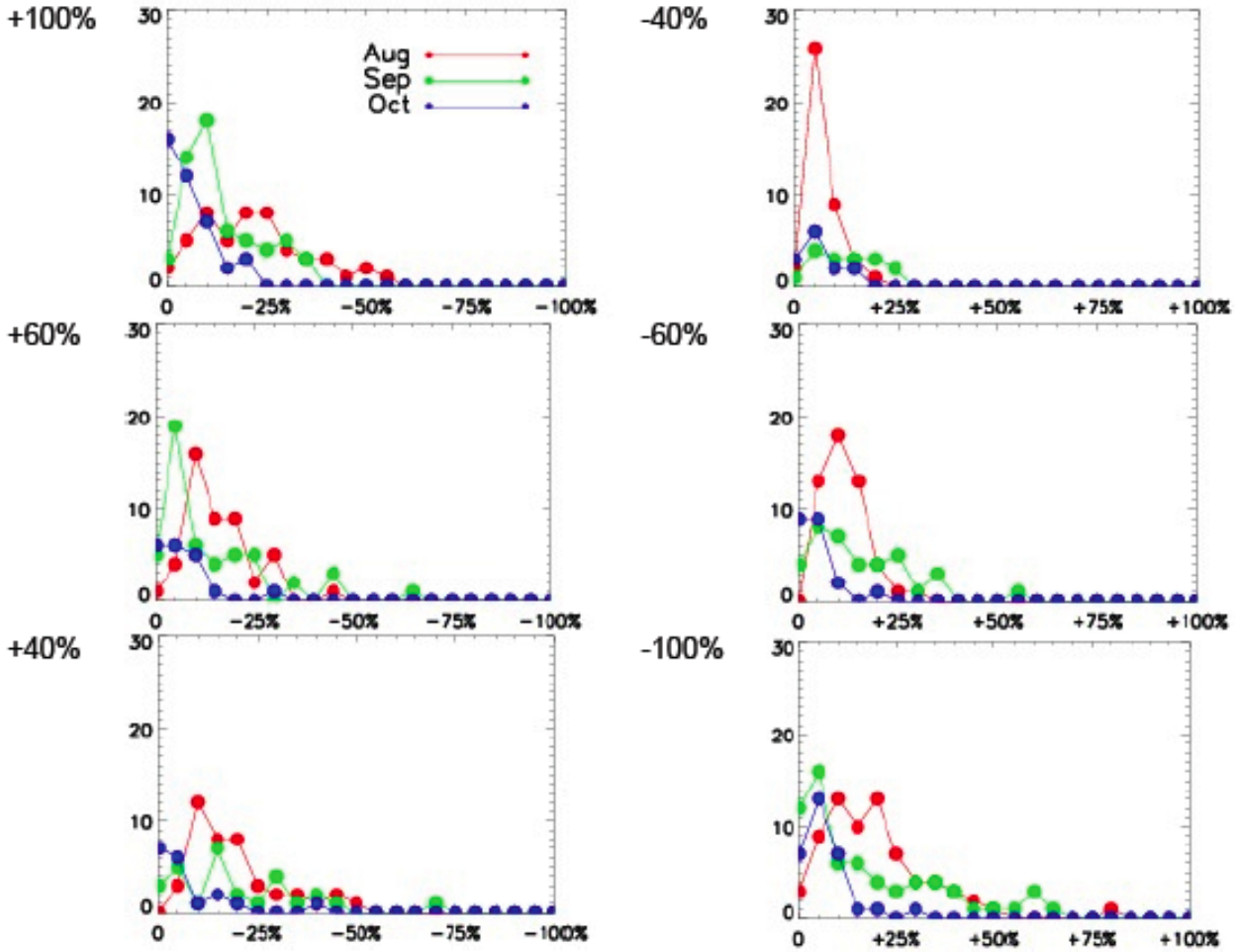

Figure 7